

# Molecular basis for interactions between an acyl carrier protein and a ketosynthase

## Supplementary Information

Jacob C. Milligan<sup>1,5</sup>, D. John Lee<sup>2,5</sup>, David R. Jackson<sup>3,5</sup>, Andrew J. Schaub<sup>3</sup>, Joris Beld<sup>2</sup>, Jesus F. Barajas<sup>1</sup>, Joseph J. Hale<sup>2</sup>, Ray Luo<sup>1</sup>, Michael D. Burkart<sup>2\*</sup>, Shiou-Chuan Tsai<sup>1,3,4\*</sup>

**Author affiliation:** <sup>1</sup>Department of Molecular Biology and Biochemistry, University of California, Irvine, CA, USA. <sup>2</sup>Department of Chemistry and Biochemistry, University of California, San Diego, La Jolla, CA, USA. <sup>3</sup>Department of Chemistry, University of California, Irvine, CA, USA. <sup>4</sup>Department of Pharmaceutical Sciences, University of California, Irvine, CA, USA. <sup>5</sup>These authors contributed equally to this work. \*email [sctsay@uci.edu](mailto:sctsay@uci.edu) or [mburkart@ucsd.edu](mailto:mburkart@ucsd.edu).

### Manuscript information:

Formatted for re-submission to *Nature Chemical Biology* as a Brief Communication.

### Supplementary Information contents:

<b>SUPPLEMENTARY TABLES</b>	<b>2</b>
<b>SUPPLEMENTARY FIGURES</b>	<b>6</b>
<b>SUPPLEMENTARY MOVIES</b>	<b>29</b>

## SUPPLEMENTARY TABLES

	AcpP-FabB (5KOF)
<b>Data collection</b>	
Wavelength (Å)	1.0
Total reflections	72648 (7131)
Unique reflections	37073 (3680)
Space group	P 1 2 <sub>1</sub> 1
Cell dimensions	
<i>a, b, c</i> (Å)	59.33, 103.92, 83.4001
$\alpha, \beta, \gamma$ (°)	90, 110.61, 90
Resolution (Å)	39.2 – 2.4 (2.486 – 2.4) <sup>a</sup>
<u><i>R</i><sub>merge</sub></u>	0.04978 (0.3953)
<u><i>R</i><sub>meas</sub></u>	0.0704 (0.559)
<i>I</i> / $\sigma$ ( <i>I</i> )	7.27 (1.76)
<i>CC</i> <sub>1/2</sub>	0.996 (0.824)
<i>CC</i> *	0.999 (0.95)
Completeness (%)	100 (100)
Redundancy	2.0 (1.9)
Wilson B-factor	40.87
<b>Refinement</b>	
Resolution (Å)	39.2 – 2.4 (2.486 – 2.4)
No. reflections	37044 (3669)
<u><i>R</i><sub>work</sub></u>	0.2080
<u><i>R</i><sub>free</sub></u>	0.2254
No. atoms	
Protein	7110
Ligands	50
<i>B</i> factors	
Protein	61.77
Ligands	75.55
Water	54.44
Ramachandran	
Favored (%)	93.4
Allowed (%)	6.0
Outliers (%)	0.6
<u>R.m.s. deviations</u>	
Bond lengths (Å)	0.006
Bond angles (°)	1.46

**Supplementary Table 1. Crystallographic data collection and refinement statistics.**

Statistics for the highest resolution shell are shown in parentheses.

Assignment	wt C <sub>8</sub> -AcpP		D38A C <sub>8</sub> -AcpP		CSP
	$\delta^1\text{H}$	$\delta^{15}\text{N}$	$\delta^1\text{H}$	$\delta^{15}\text{N}$	
03I	8.696	121.850	8.546	122.170	0.111 *
04E	8.656	118.955	8.435	114.847	0.436 *
05E	7.896	117.827	7.910	117.618	0.023
06R	8.395	120.275	8.360	120.145	0.028
07V	8.965	119.456	9.023	119.418	0.041
08K	8.271	117.389	8.245	117.303	0.020
09K	8.318	120.854	8.247	121.267	0.065
10I	7.659	119.721	7.760	119.822	0.072
11I	8.356	119.228	8.436	119.181	0.057
12G	8.503	105.573	8.421	105.325	0.063
13E	8.244	120.501	8.237	120.547	0.007
14Q	8.463	117.753	8.669	117.155	0.157 *
15L	8.136	113.771	8.264	113.924	0.092
16G	7.849	110.235	7.800	110.242	0.035
17V	7.924	114.922	7.903	114.493	0.045
18K	8.589	123.293	8.594	123.126	0.017
19Q	8.835	123.095	8.831	123.109	0.003
20E	9.445	116.889	9.466	116.943	0.016
21E	7.919	117.279	7.940	117.229	0.016
22V	7.576	122.757	7.596	122.659	0.017
23T	7.371	115.887	7.352	115.721	0.021
24N	8.629	119.086	8.642	119.048	0.010
25N	8.147	112.280	8.150	112.200	0.008
26A	7.349	123.231	7.372	123.299	0.018
27S	9.987	117.289	9.993	117.280	0.004
28F	7.595	125.331	7.587	125.421	0.011
29V	8.817	117.002	8.800	117.013	0.012
30E	8.342	117.098	8.326	117.066	0.012
31D	7.826	114.280	7.831	114.336	0.007
32L	7.411	115.707	7.428	115.600	0.016
33G	7.270	106.818	7.259	106.727	0.012
34A	8.512	123.052	8.566	123.064	0.038
35D	9.370	123.501	7.934	123.393	1.015 *
36S	8.691	113.447	8.775	114.168	0.093
37L	8.218	123.919	8.324	122.338	0.174 *
38D	8.379	120.014	7.586	121.092	0.571 **
39T	8.228	112.167	8.312	111.067	0.124 *
40V	7.272	121.431	7.359	122.051	0.087
41E	7.860	119.358	7.813	119.381	0.033
42L	8.450	121.751	8.340	121.838	0.078
43V	8.020	119.376	8.072	119.709	0.049
44M	7.792	117.246	7.801	117.266	0.007
45A	8.181	121.772	8.157	121.955	0.025

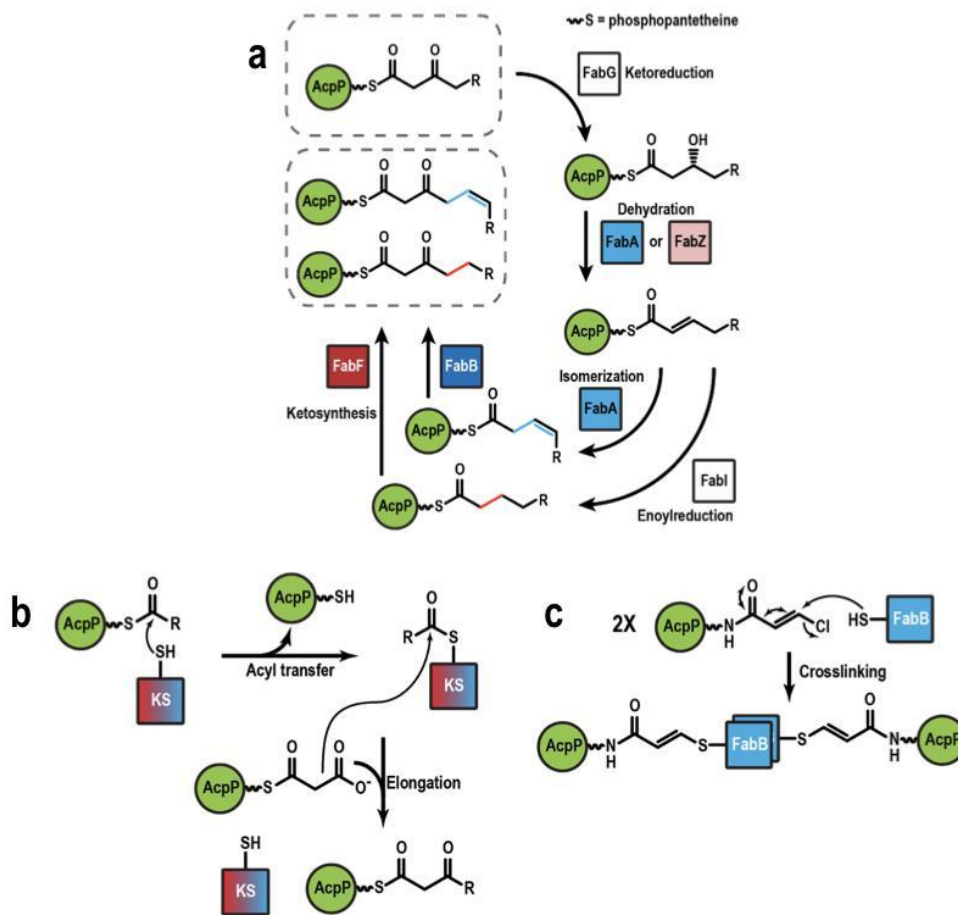
46L	8.430	120.866	8.432	120.820	0.005
47E	8.743	120.243	8.715	120.149	0.022
48E	7.896	117.285	7.904	117.193	0.011
49E	7.990	120.008	8.038	119.533	0.058
50F	7.840	111.805	7.843	111.827	0.003
51D	7.909	122.744	7.923	122.880	0.017
52T	8.083	112.548	8.093	112.754	0.022
53E	8.156	122.920	8.087	122.596	0.058
54I	10.406	129.131	10.382	129.154	0.017
55P					
56D	8.950	125.628	8.961	125.533	0.012
57E	9.299	116.557	9.311	116.572	0.009
58E	7.259	116.260	7.260	116.260	0.001
59A	8.219	123.159	8.284	123.274	0.047
60E	7.609	112.545	7.626	112.655	0.016
61K	7.064	114.423	7.085	114.498	0.017
62I	7.672	123.047	7.688	123.118	0.013
63T	8.083	112.548	8.021	112.375	0.047
64T	7.272	110.705	7.237	110.633	0.026
65V	8.040	121.757	8.023	121.648	0.016
66Q	8.735	118.250	8.723	118.148	0.013
67A	7.823	119.611	7.814	119.572	0.007
68A	7.997	123.042	8.004	122.981	0.008
69I	8.166	119.500	8.167	119.481	0.002
70D	9.163	119.401	9.144	119.297	0.017
71Y	8.203	122.028	8.204	121.890	0.014
72I	8.239	121.178	8.180	121.275	0.043
73N	8.880	118.545	8.849	118.456	0.024
74G	7.884	105.384	7.838	105.132	0.041
75H	7.692	119.015	7.656	118.397	0.066

**Supplementary Table 2. Chemical Shift Tables for wt and D38A C<sub>8</sub>-AcpP.** Chemical shift assignments are reported for wt C<sub>8</sub>-AcpP and D38A C<sub>8</sub>-AcpP (amide replacement of the phosphopantetheine thioester). CSP values between these two species are reported, indicating good chemical shift agreement between the two. \* denotes residues with a > 0.100 CSP. \*\* indicates the mutation site. 21E and 48E are aliased with each other in both species, and omitted in Figure 3.

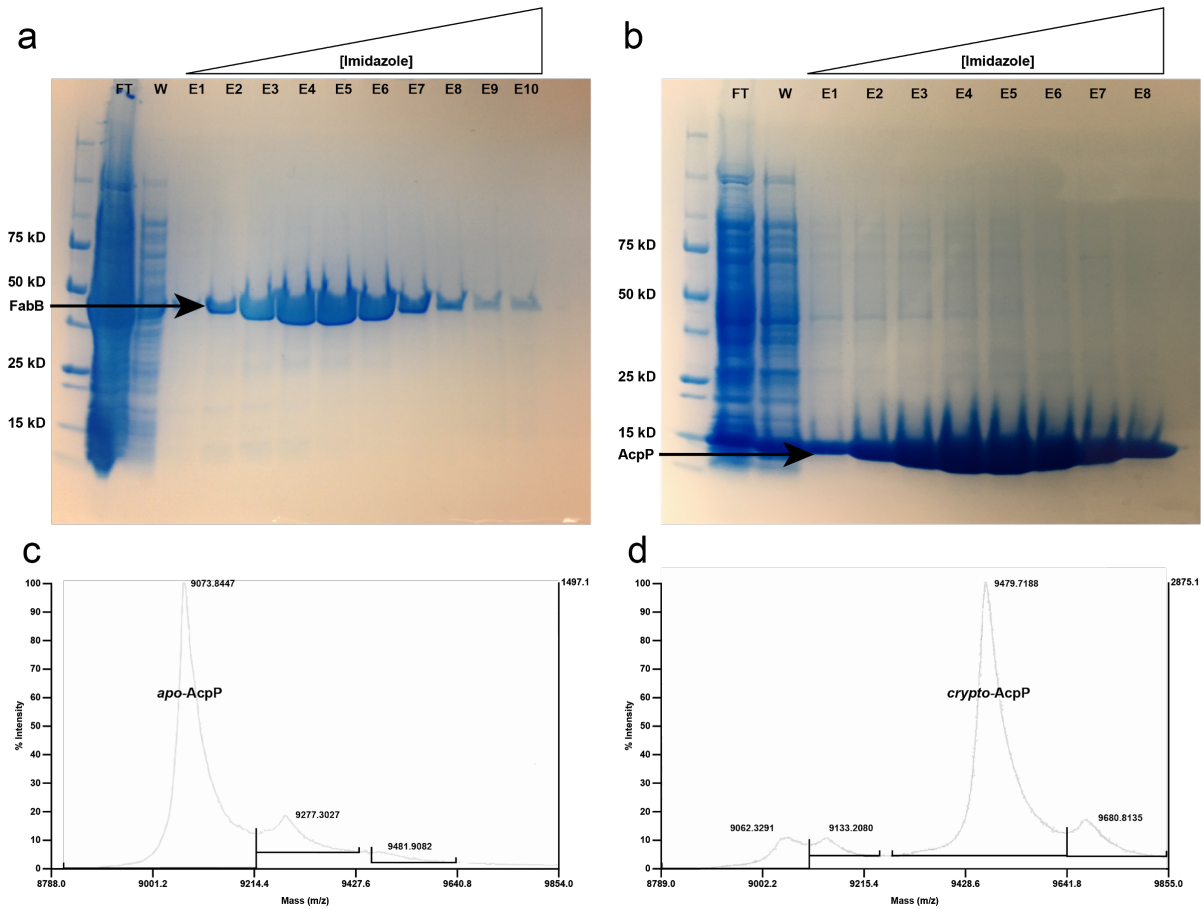
	K <sub>d</sub> NMR Titration with FabB			Complementation UFA Fraction, 17 °C		Complementation UFA Fraction, 25 °C		Complementation UFA Fraction, 37 °C	
	wt	D38A		wt	D38A	wt	D38A	wt	D38A
AcpP			AcpP						
M <sub>Kd</sub>	37.6 μM	167 μM	M <sub>UFA</sub>	0.519	0.428	0.473	0.393	0.417	0.400
SD <sub>Kd</sub>	6.6 μM	15 μM	SD <sub>UFA</sub>	0.019	0.016	0.005	0.010	0.002	0.004
N	10 observations each		N	4 cultures each		4 cultures each		4 cultures each	
Two-tailed unpaired t-test (Student's test)									
t	24.9697		t	7.4589		14.6946		7.2843	
DF	18		DF	6		6		6	
P value	< 0.0001		P value	0.0003		< 0.0001		0.0003	
Cohen's <i>d</i> for independent groups $d = (M_2 - M_1)/SD_{pooled}$									
Cohen's <i>d</i>	11.1670		Cohen's <i>d</i>	5.2744		10.3914		5.1517	

**Supplementary Table 3. Statistical analysis of K<sub>d</sub> and fatty acid extraction values.**

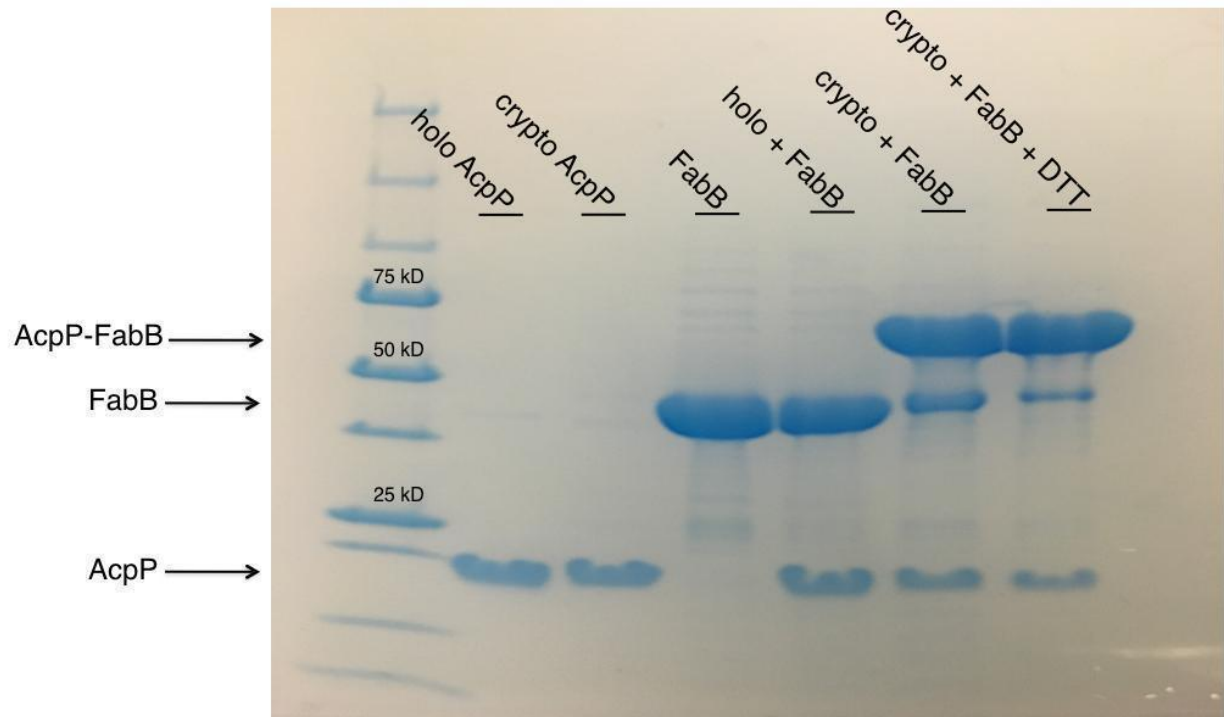
## SUPPLEMENTARY FIGURES



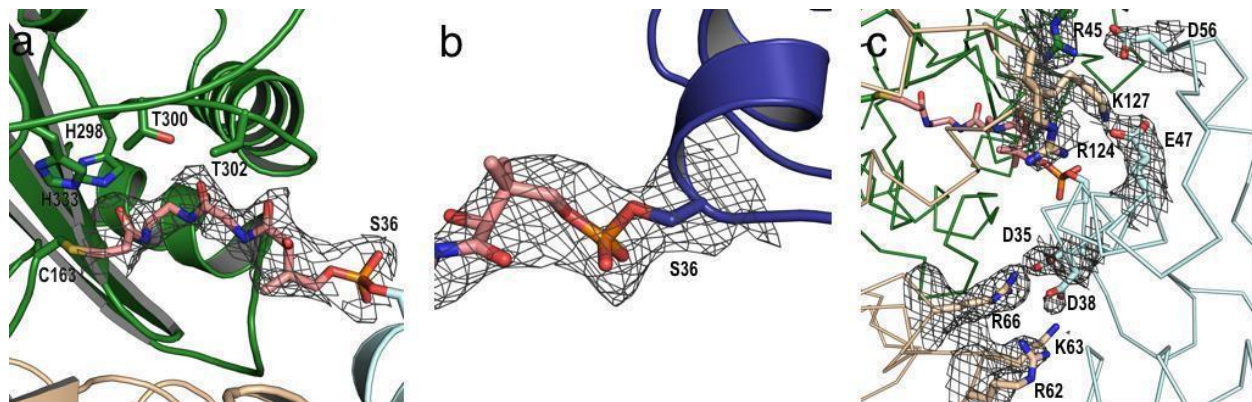
**Supplementary Figure 1. Biosynthesis of fatty acids in *E. coli* and mechanism-based crosslinking.** (a) Overview of biosynthetic pathway. FabA and FabB, in blue, produce and elongate unsaturated fatty acids. FabZ and FabF, in red, produce and elongate saturated fatty acids. FabG and FabI, in white, perform appropriate reductions to complete the cycle. These cycles are iterated to produce full-length fatty acid chains. R = even length acyl chains between 0 and 14 carbons (yielding final products 16 and 18 carbons long) varying in length based on how many upstream iterations of the cycle have already occurred. (b) mechanism for ketosynthase reaction and enzyme turnover. (c) mechanism-based crosslinking reaction.



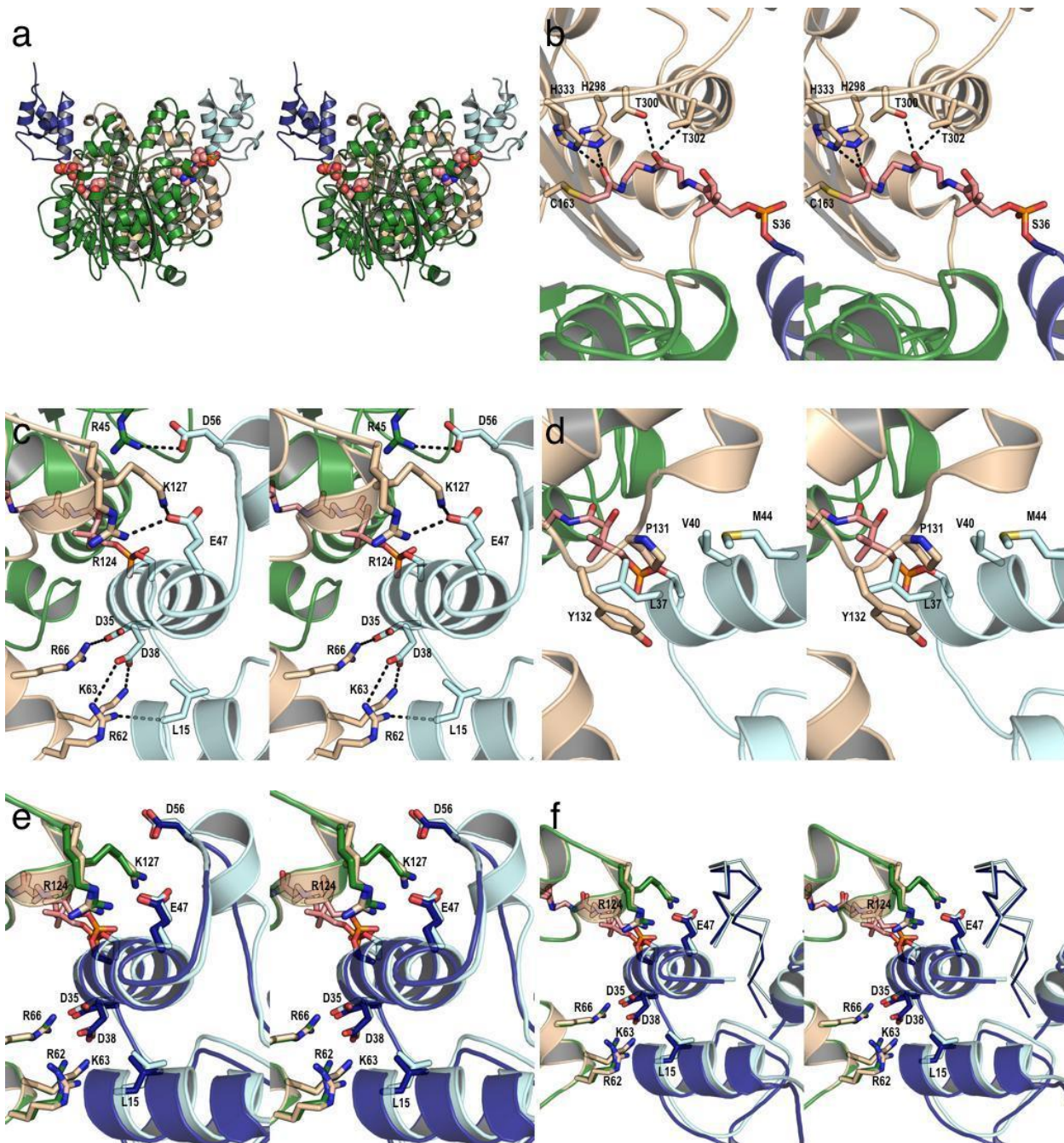
**Supplementary Figure 2. Protein purification and AcpP loading.** (a)(b) SDS-PAGE gels showing fractions from FabB Ni<sup>2+</sup> affinity column (a) and AcpP Ni<sup>2+</sup> affinity column (b). MALDI-TOF mass spectrum of *apo* AcpP (calculated molecular weight of 9052 Da). (d) MALDI-TOF mass spectrum of *crypto* AcpP (calculated molecular weight of 9466 Da).



**Supplementary Figure 3. AcpP-FabB crosslinking reaction.** SDS-PAGE gel confirming covalent crosslinking of *crypto* AcpP and FabB. DTT was added to the reaction to maintain an ideal oxidative state for crosslinking.

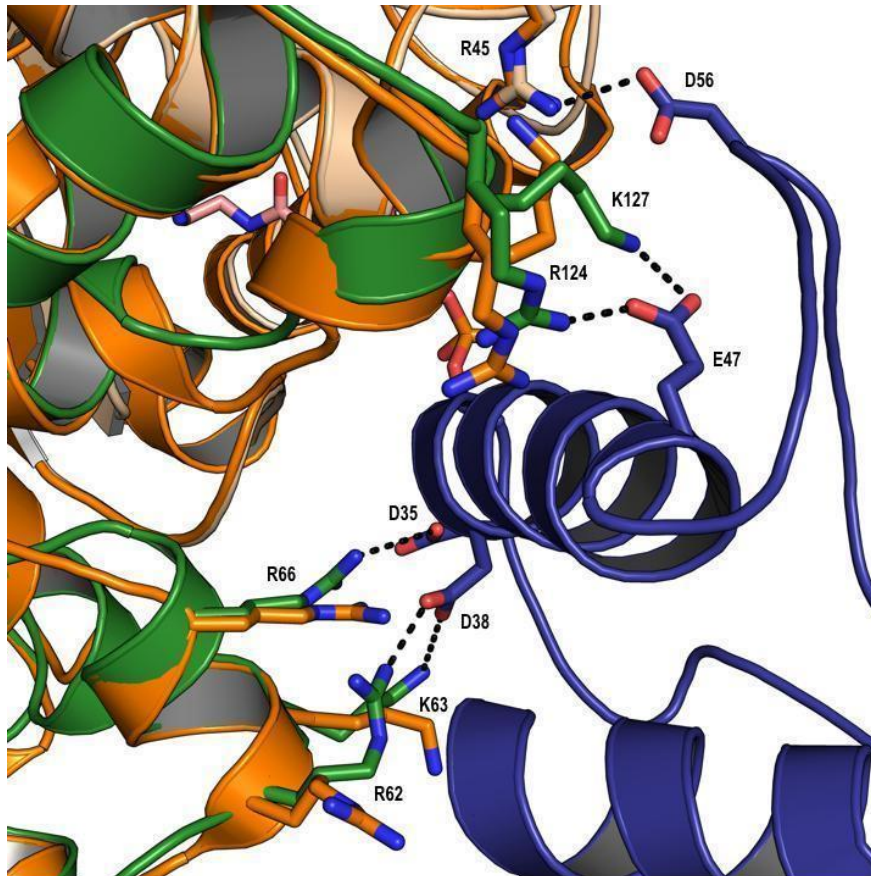


**Supplementary Figure 4. Composite omit maps at 1.0 sigma.** (a) crosslinker in the FabB active site with AcpP shown in light cyan and FabB shown in dark green and light tan. (b) crosslinker connection with AcpP, with AcpP shown in dark blue. (c) AcpP-FabB interface residues.

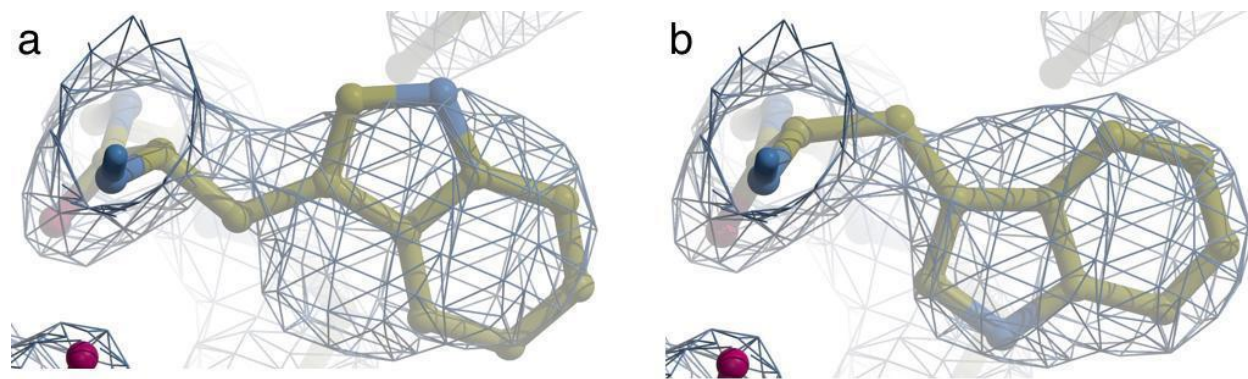


**Supplementary Figure 5. Stereo images of AcpP-FabB structure.** (a) overall structure of the AcpP-FabB complex, with the FabB monomers shown in green and tan, the AcpPs shown in dark blue and cyan, and the crosslinker shown in colored spheres. (b) FabB active site interactions with the crosslinker. (c) AcpP-FabB interface salt bridges. (d) AcpP-FabB interface hydrophobic interactions. (e) overlay of interfaces. (f) overlay of interfaces with helix III shown in ribbon

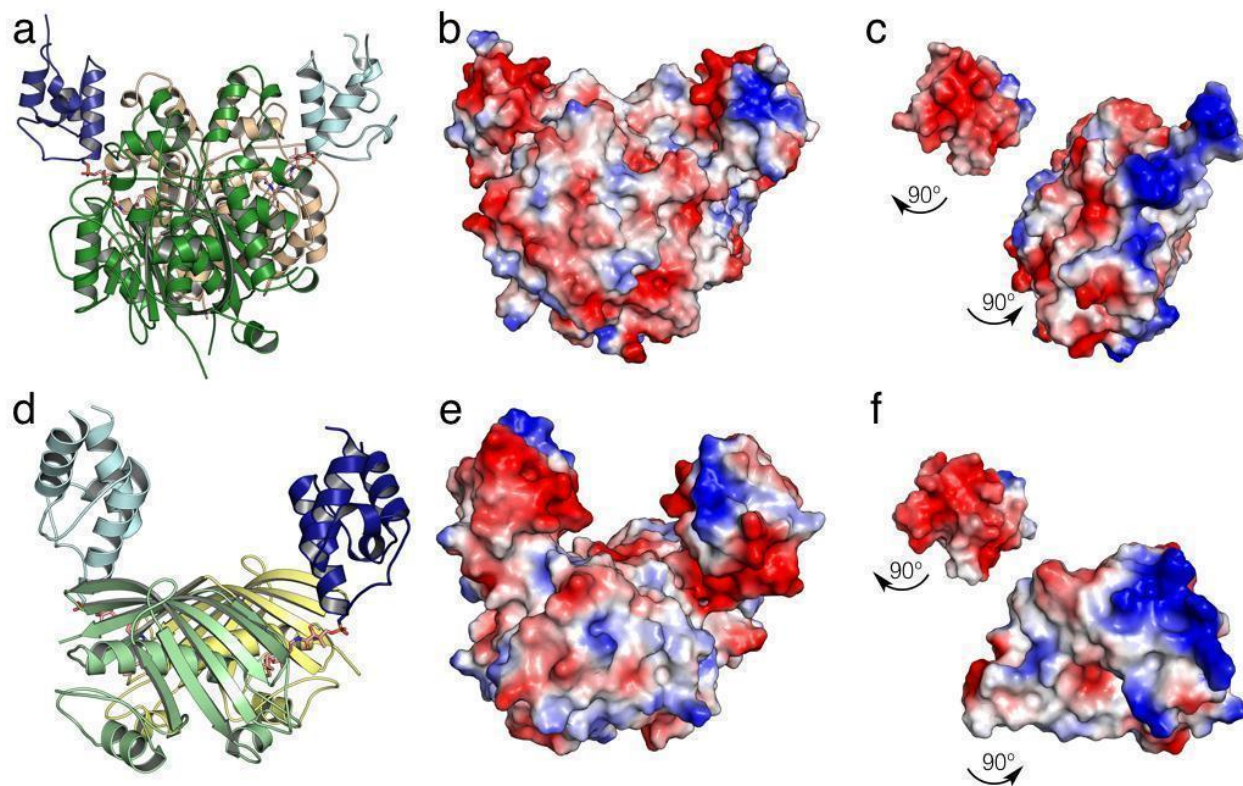
representation to highlight differences in backbone structure.



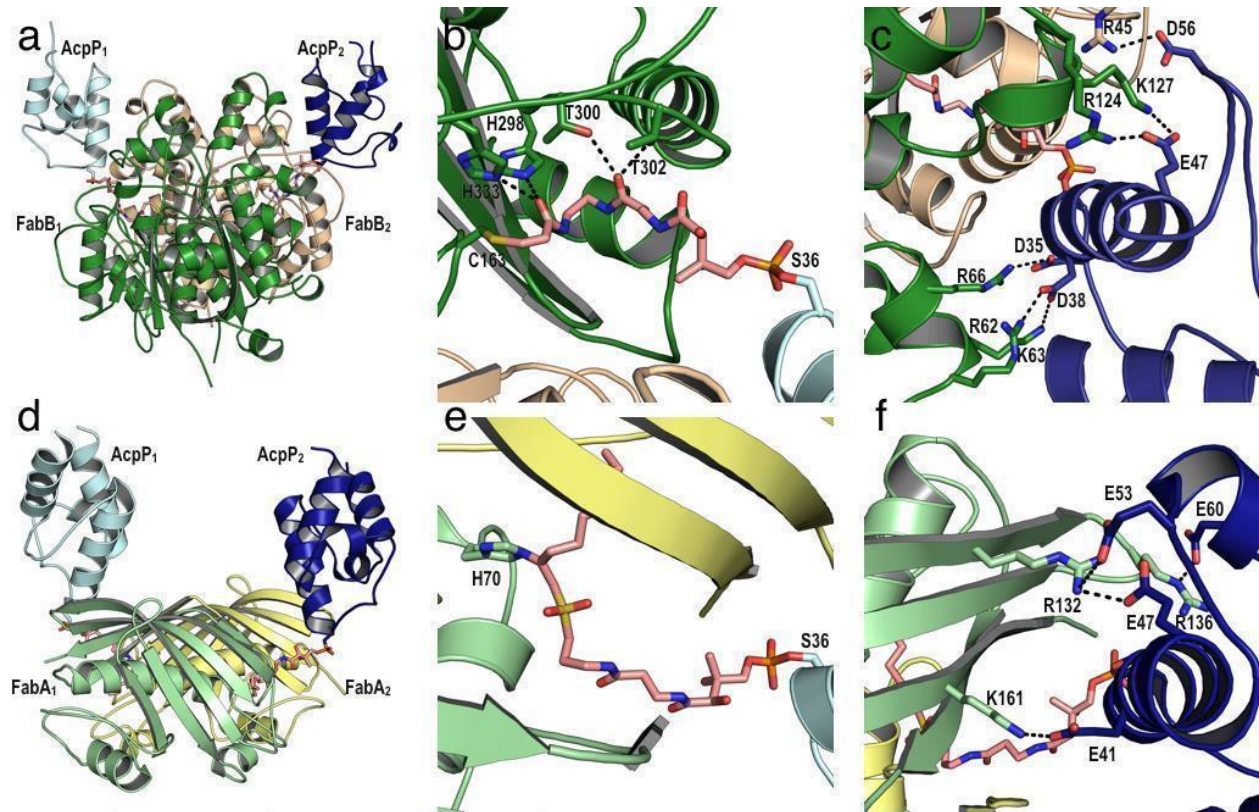
**Supplementary Figure 6. FabB surface changes upon AcpP binding.** Overlay of AcpP-FabB complex structure (green, light tan, and dark blue) with the apo FabB structure (orange).



**Supplementary Figure 7. Alternate conformations of Trp 49 in one monomer of FabB. a,** conformation deposited in the PDB. **b,** alternate conformation.

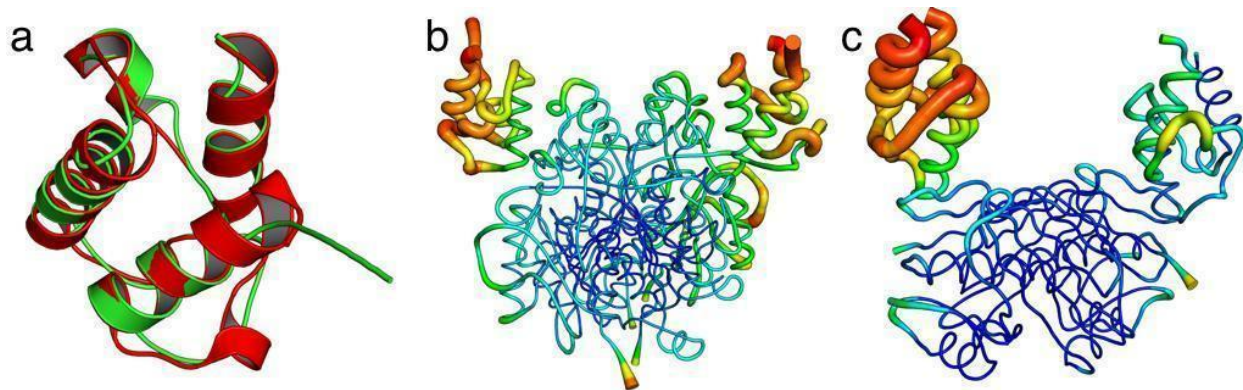


**Supplementary Figure 8. Surface electrostatics of AcpP-FabB and AcpP-FabA.** (a) AcpP-FabB. (b) AcpP-FabB surface charges. (c) surfaces charges at the AcpP-FabB interface. (d) AcpP-FabA. (e) AcpP-FabA surface charges. (f) surfaces charges at the AcpP-FabA interface.

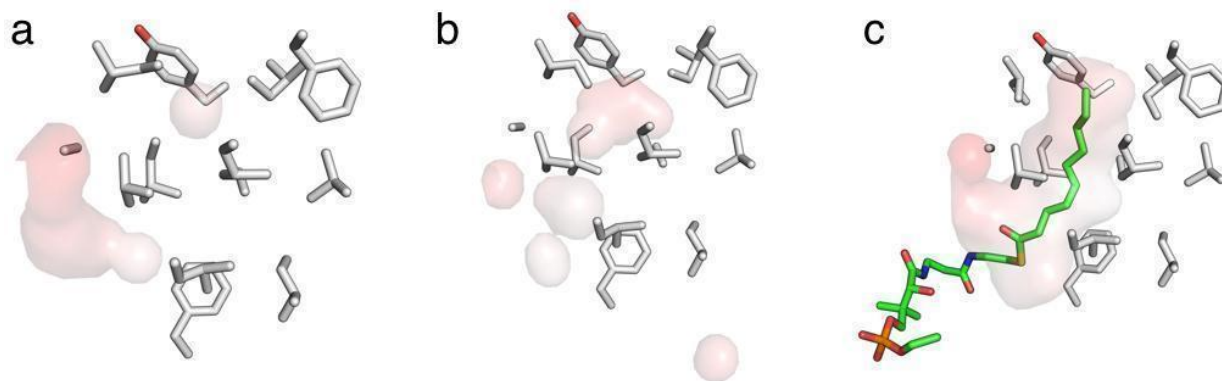


**Supplementary Figure 9. Comparison of AcpP-FabB and AcpP-FabA complex structures.**

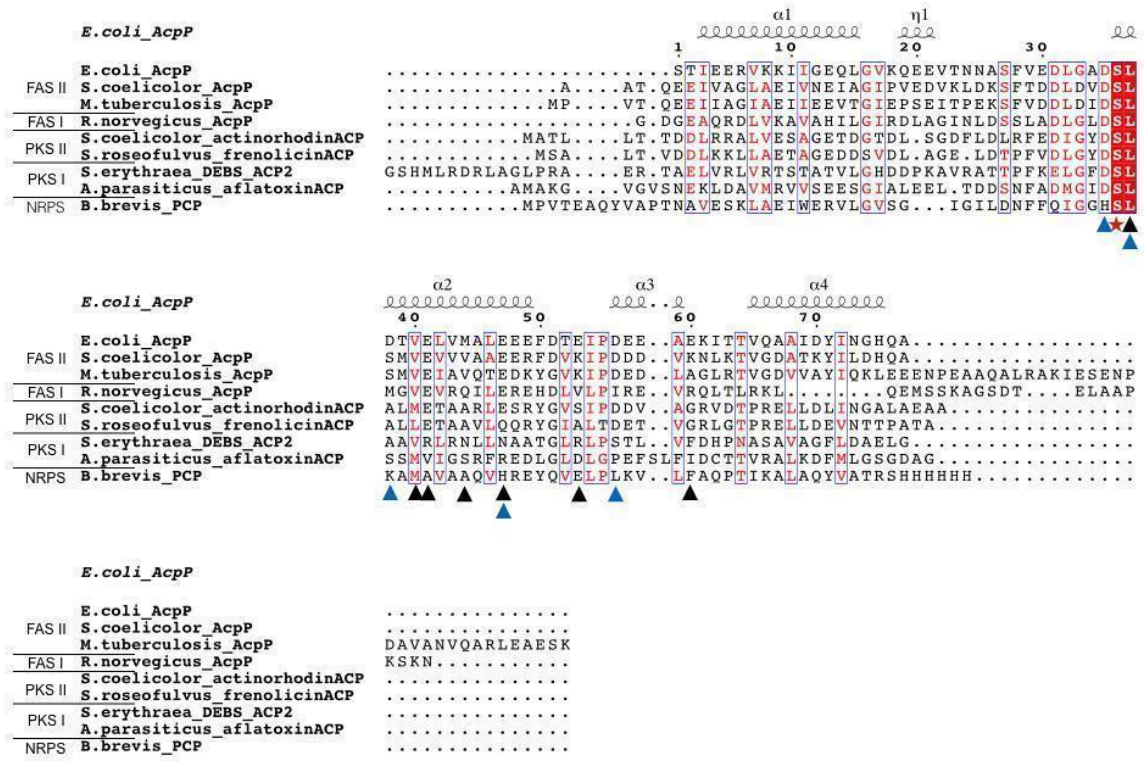
(a) Overall AcpP-FabB complex structure, with the FabB monomers shown in dark green and light tan, the AcpP monomers shown in dark blue and light cyan, and the crosslinker in pink. (b) FabB active site interactions with the crosslinker. (c) AcpP-FabB interface. (d) Overall AcpP-FabA complex structure, with the FabA monomers shown in light green and light yellow, the AcpP monomers shown in dark blue and light cyan, and the crosslinker in pink. (e) FabA active site interactions with the crosslinker. (f) AcpP-FabA interface



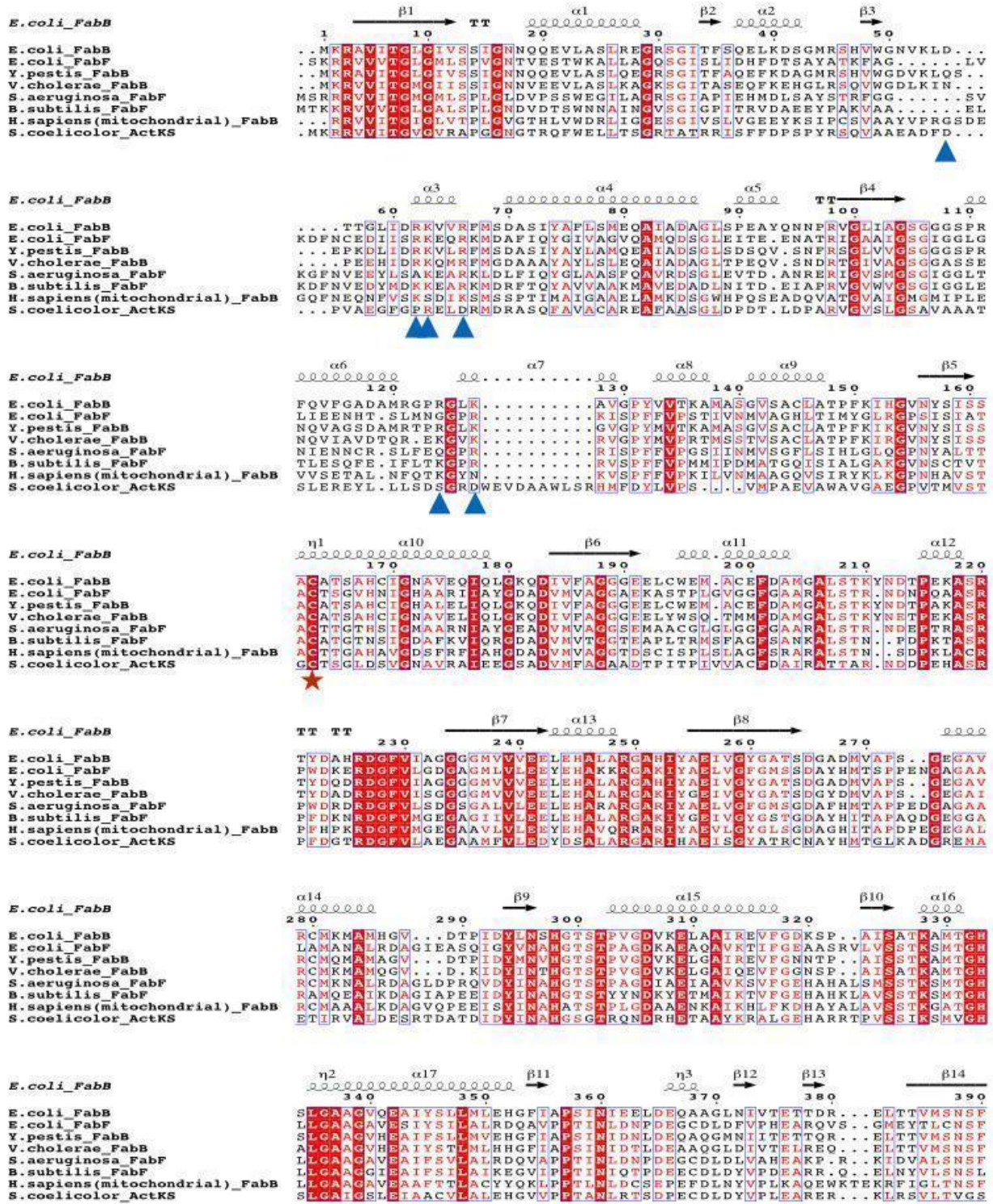
**Supplementary Figure 10. AcpP comparison between AcpP-FabB and AcpP-FabA.** (a) Overlay of AcpP from AcpP-FabA (red) and from AcpP-FabB (green). (b)(c) B-factor putty representation of AcpP-FabB (b) and AcpP-FabA (c) where thin, blue tubes correspond to low B-factors and thicker, darker red tubes correspond to higher B-factors.



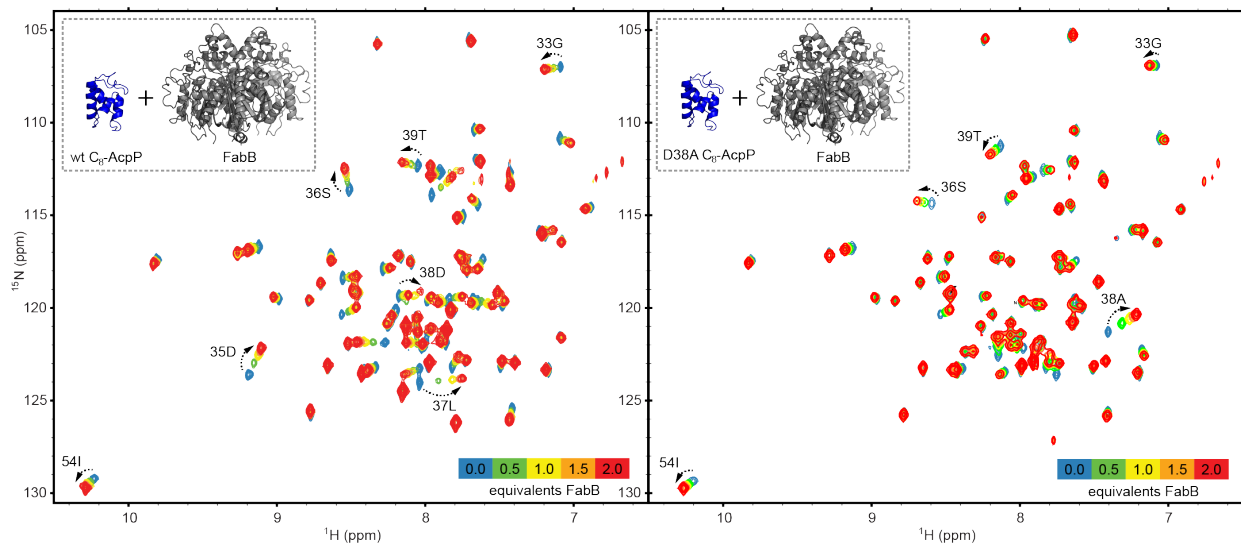
**Supplementary Figure 11. AcpP substrate pocket comparison between AcpP-FabA, AcpP-FabB, and octanoyl-AcpP (2FAE) shows chain flipping and substrate delivery. (a) AcpP substrate pocket from AcpP-FabA. (b) AcpP substrate pocket from AcpP-FabB. (c) AcpP substrate pocket from octanoyl-AcpP.**



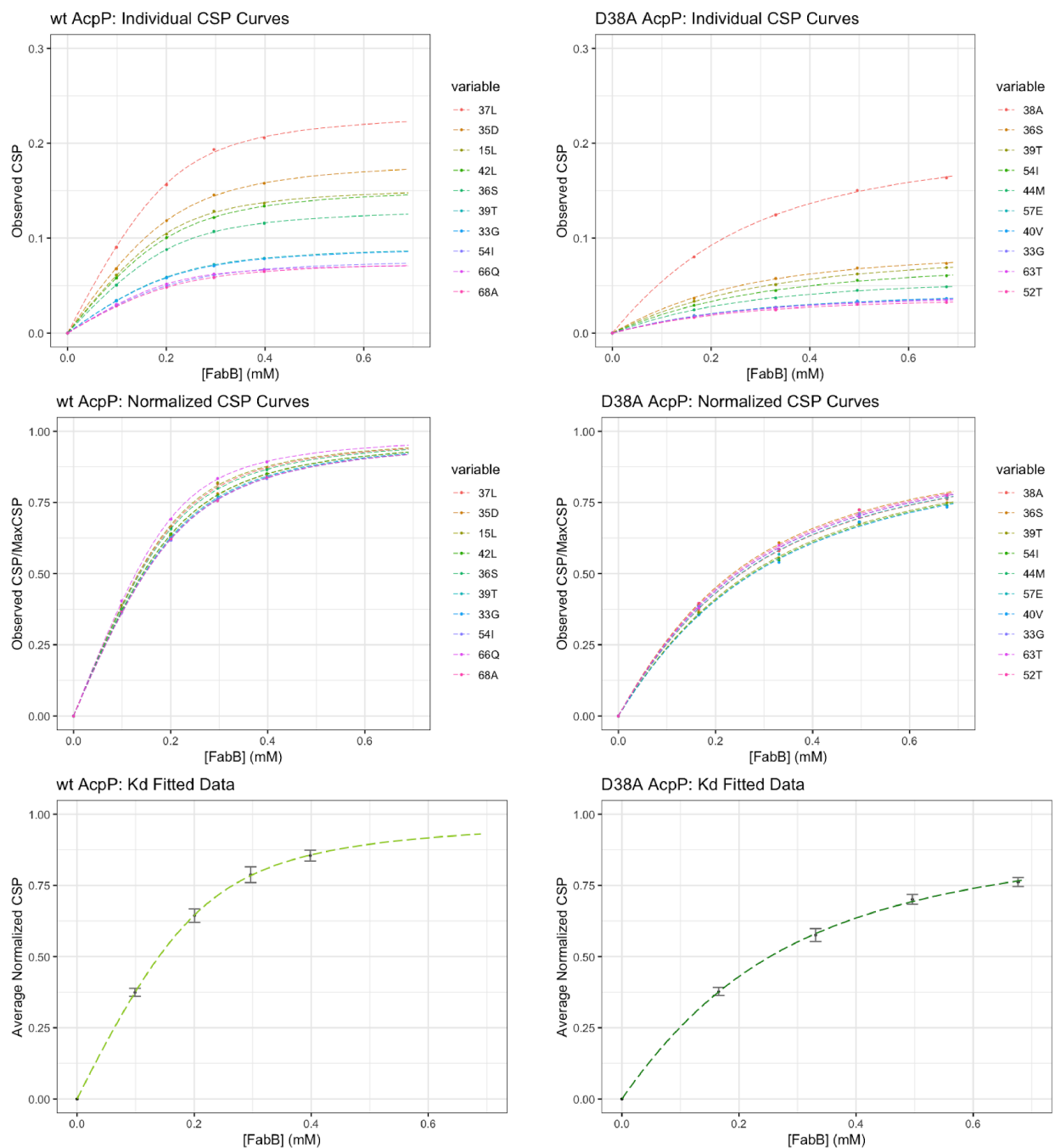
**Supplementary Figure 12. Sequence alignment of carrier proteins. Red star: PPT attachment site. Black Triangle: AcpP-FabA interface residues. Blue triangle: AcpP-FabB interface residues.**



Supplementary Figure 13. Sequence alignment of ketosynthases. Red star: Active site. Blue triangle: AcpP-FabB interface residues.



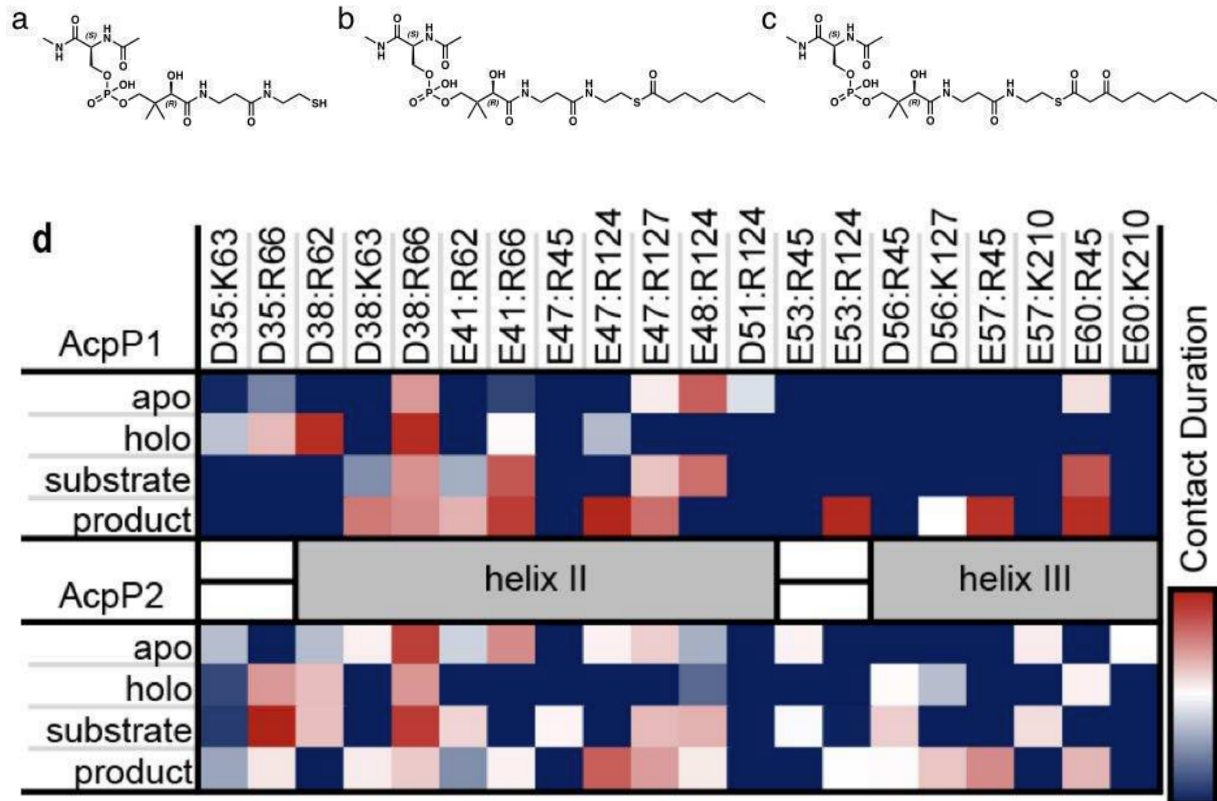
**Supplementary Figure 14. NMR studies of the AcpP-FabB complex.**  $^1\text{H}$ ,  $^{15}\text{N}$ -HSQC titration experiments of wt AcpP (at left) and D38A AcpP (at right) against increasing concentrations of FabB.



**Supplementary Figure 15. CSP Derived  $K_d$  Curves.** Top: CSP curves for 10 non-aliased residues with the largest observed CSPs for wt and D38A AcpP titrated with FabB. Mid: Normalized CSP curves (Observed CSP/MaxCSP - determined via fitting described in Online Methods). Bottom: Average Normalized CSP curves. Error bars are +/- one standard deviation for normalized CSP value. Observed wt AcpP concentration: 0.21 mM;  $K_d$  calculated to be 37.6 ±

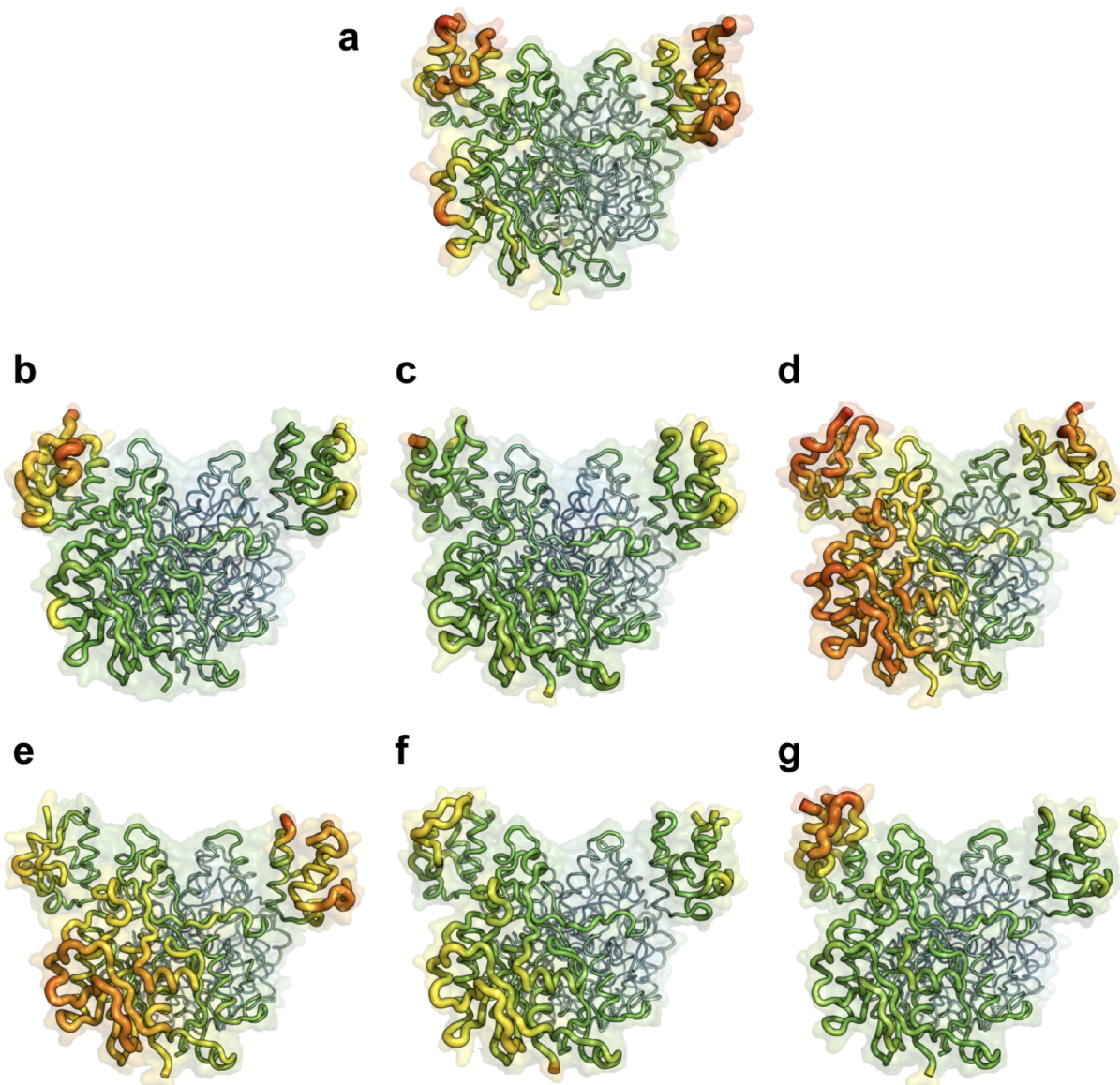
6.6  $\mu\text{M}$ . Observed D38A AcpP concentration: 0.17 mM;  $K_d$  calculated to be  $167 \pm 15 \mu\text{M}$ ,  $P < 0.0001$ .





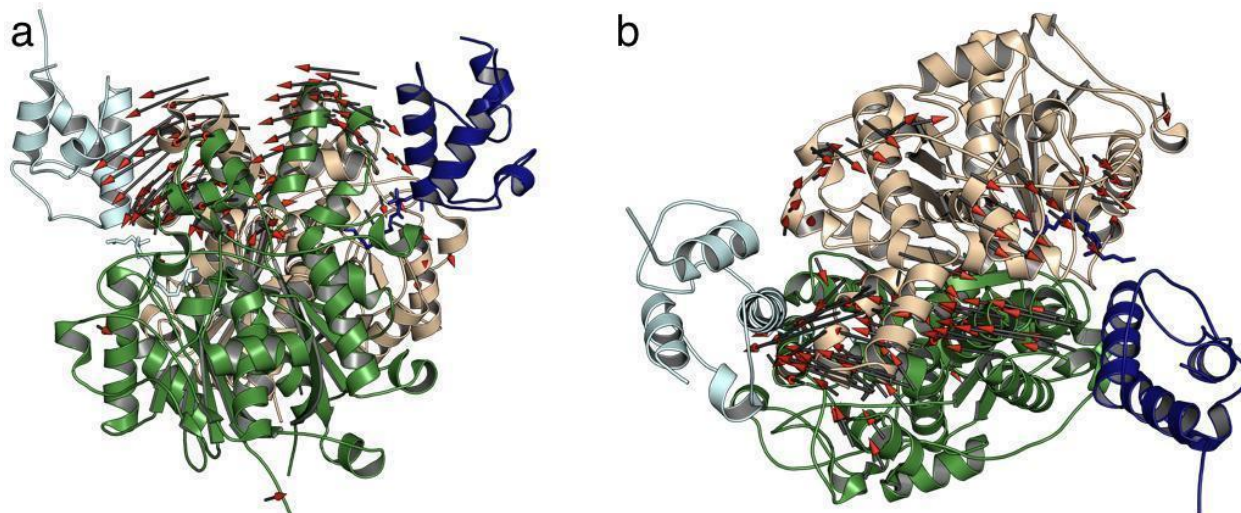
**Supplementary Figure 17. Salt bridge duration in MD simulations of AcpP-FabB**

**complexes.** (a) holo-ACP. (b) octanoyl-ACP, “substrate”. (c) 3-oxodecyl-ACP, “product”. These acetyl and N-methyl capped structures were used for force field generation using the R.E.D. Server and Gaussian. (d) The duration of MD-observed salt bridges between different AcpP species and FabB. Contact durations are colored on a spectrum from persisting for 0% of the simulation (blue) to 100% of the simulation (red).

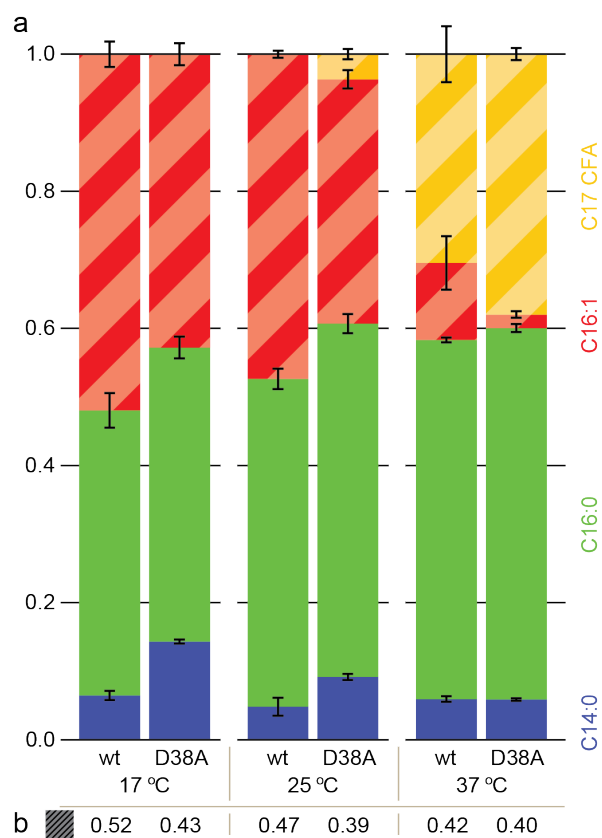


**Supplementary Figure 18. A comparison of MD derived RMSFs and crystallographic B-factors.** All the above structures are displayed as putty, with higher RMSF/ B-factor values shown in red with increased thickness, and lower values shown in blue with decreased thickness. All MD structures are the average structure generated from the 1000 frames representing 140 to 150 ns. The RMSF MD structures are normalized with the crystallographic B-factors for comparison purposes. (a) Crystallographic structure for reference. Higher disorder is observed in FabB2 of the homodimer. (b) Both AcpPs in apo state. (c) Both AcpPs loaded with C8-substrate. (d) AcpP1 of the homodimer. (e) AcpP2 of the homodimer. (f) AcpP1 of the heterodimer. (g) AcpP2 of the heterodimer.

(left) and AcpP2 (right) loaded with C8-substrate and C8-product, respectively. (e) Both AcpPs in holo state. (f) Both AcpPs loaded with C8-product. (g) AcpP1 (left) and AcpP2 (right) loaded with C8-product and C8-substrate, respectively.



**Supplementary Figure 19. Porcupine figures showing the symmetric rocking motion obtained from the trajectory of the first mode from the principal component analysis.** The vectors were generated using the beginning and final structures of the first mode trajectories, and the vectors were overlaid on the crystal structure for ease of visualization.



**Supplementary Figure 20.** (a) Specific isolated fatty acids reported in figure 3c. Averages are over four replicates for each condition. (b) Unsaturated fatty acid fraction, including cyclopropyl-C17 (derived from C16:1).

## **SUPPLEMENTARY MOVIES**

### **Movie S1. Principal component analysis of AcpP-FabB molecular dynamics simulations.**

The movie shows the first three modes from the principal component analysis. Mode 1 is a twisting of the AcpPs along the center axis of the FabB homodimer. Mode 2 is a scissoring of the AcpPs along the same axis. Mode 3 is wagging of the AcpPs along the same axis. The two FabB monomers are shown in dark green and light tan, and the two AcpPs are shown in light cyan and dark blue.

### **Movie S2. Principal component analysis of AcpP-FabB molecular dynamics simulations.**

The same results shown in Movie S1 are shown again from a perpendicular viewing angle.